

Geophysical Research Letters[®]



RESEARCH LETTER

10.1029/2025GL115586

Key Points:

- LOw Frequency ARray has the unique ability to simultaneously perform cosmic-ray and lightning imaging observations to use for atmospheric science
- The general agreement between the charge structure heights from two observations confirms the consistency of these two independent methods
- A triple-layer charge structure is found with a dominant lower positive charge, in contrast to typical thunderstorms

Supporting Information:

Supporting Information may be found in the online version of this article.

Correspondence to:

T. N. G. Trinh,
ttnghia@ctu.edu.vn

Citation:

Trinh, T. N. G., Scholten, O., van Loon, R., Hare, B. M., Assink, J. D., Bouma, S., et al. (2025). Thunderstorm charge distribution determination using cosmic rays induced air showers and lightning imaging at LOFAR. *Geophysical Research Letters*, 52, e2025GL115586. <https://doi.org/10.1029/2025GL115586>

Received 17 OCT 2024

Accepted 31 MAR 2025

Author Contributions:

Data curation: G. K. Krampah, S. ter Veen

Formal analysis: T. N. G. Trinh, O. Scholten

Investigation: T. N. G. Trinh, O. Scholten

Resources: R. van Loon












Writing – original draft: T. N. G. Trinh, O. Scholten

Writing – review & editing: T. N. G. Trinh, O. Scholten, R. van Loon, B. M. Hare, J. D. Assink, S. Bouma, S. Buitink, A. Corstanje, S. Cummer, M. Desmet, J. Dwyer, H. Falcke, J. R. Hörandel, T. Huege, N. Karastathis, P. Laub, N. Liu, M. Lourens, K. Mulrey, A. Nelles, H. Pandya, C. Sterpka, K. Terveer, S. Thoudam, P. Turekova

© 2025. The Author(s).

This is an open access article under the terms of the [Creative Commons Attribution License](#), which permits use, distribution and reproduction in any medium, provided the original work is properly cited.

Thunderstorm Charge Distribution Determination Using Cosmic Rays Induced Air Showers and Lightning Imaging at LOFAR

T. N. G. Trinh¹ , O. Scholten^{2,3} , R. van Loon⁴, B. M. Hare^{2,5} , J. D. Assink⁴ , S. Bouma⁶, S. Buitink³, A. Corstanje³, S. Cummer⁷ , M. Desmet³, J. Dwyer⁸, H. Falcke^{9,10}, J. R. Hörandel⁹, T. Huege¹¹, N. Karastathis¹¹, G. K. Krampah³, P. Laub⁶ , N. Liu⁸ , M. Lourens⁵ , K. Mulrey⁹, A. Nelles^{6,12}, H. Pandya³ , C. Sterpka⁸ , K. Terveer⁶, S. Thoudam¹³, P. Turekova^{2,5} , and S. ter Veen⁵

¹Physics Education Department, School of Education, Can Tho University, Can Tho City, Viet Nam, ²Kapteyn Astronomical Institute, University of Groningen, Groningen, The Netherlands, ³Interuniversity Institute for High-Energy, Vrije Universiteit Brussel, Brussels, Belgium, ⁴Royal Netherlands Meteorological Institute (KNMI), De Bilt, The Netherlands, ⁵Netherlands Institute for Radio Astronomy (ASTRON), Dwingeloo, The Netherlands, ⁶Erlangen Centre for Astroparticle Physics (ECAP), Friedrich-Alexander-Universität Erlangen-Nürnberg, Erlangen, Germany, ⁷Department of Electrical and Computer Engineering, Duke University, Durham, NC, USA, ⁸Department of Physics and Astronomy, and Space Science Center (EOS), University of New Hampshire, Durham, NH, USA, ⁹Department of Astrophysics/IMAPP, Radboud University Nijmegen, Nijmegen, The Netherlands, ¹⁰Nikhef, Science Park Amsterdam, Amsterdam, The Netherlands, ¹¹KIT, Karlsruhe, Germany, ¹²Deutsches Elektronen-Synchrotron DESY, Zeuthen, Germany, ¹³Department of Physics, Khalifa University, Abu Dhabi, United Arab Emirates

Abstract The LOw Frequency ARray (LOFAR) radio telescope possesses the unique capability to measure ultra-high energy cosmic rays as well as image lightning discharges. This study presents a comparison between the inferred thunderstorm charge structures derived from cosmic-ray measurements and from lightning flashes. Our results show a basic triple-layered distribution: a positive upper layer, a main negative layer, and a positive lower layer. However, our cosmic-ray measurement shows a bottom-heavy structure, where the charge in the upper positively charged layer is smaller than that in the lower one. This is consistent with practically all lightning observations with LOFAR, showing well-developed negative leader structures at altitudes below those where positive leaders are seen. This is very different from the vast majority of thundercloud charge structures seen around the world.

Plain Language Summary The LOw Frequency ARray radio telescope can measure radio signals from extensive air showers induced by cosmic rays during thunderstorms, helping us understand the charge distribution within thunderclouds. It can also capture images of lightning to study the charge structures. In this study, we compared the charge structures as determined by cosmic-ray measurements and lightning flashes. For one event, both methods show a general agreement in the heights of the charge layers. In addition, the suspicion is confirmed that the charge structure of Dutch thunderstorms is different from the majority seen around the world. Usually the charge is distributed in three layers: a large positive charge at the top, a negative charge in the middle, and another weak positive charge at the bottom, referred to as a top-heavy charge distribution. However, our measurements indicate that Dutch thunderstorms are generally bottom-heavy, where the upper positive charge is weaker than the lower one.

1. Introduction

Understanding the charge structure of thunderclouds and the resulting electric field is crucial for lightning research, yet such measurements are challenging due to their dynamic nature. One, long standing, issue is that for the thunderstorms imaged by LOw Frequency ARray (LOFAR) (called Dutch thunderstorms) one consistently observes evidence for a different structure as compared to the large majority of thunderstorms measured around the world (Rakov & Uman, 2007). In Dutch thunderstorms, one observes a very well-developed negative leader structure at altitudes below that of the positive leaders. Results of balloon measurements in the US often show a basic triple-layered charge distribution: a stronger positive upper layer, a main negative layer, and a weaker positive lower layer, that is, a top-heavy charge distribution (Marshall & Stolzenburg, 1998; Rutledge et al., 1993;

Stolzenburg et al., 1998), see additional references in Dwyer and Uman (2014). This is consistent with LMA measurements across the US, showing most often a well-developed negative leader structure above positive leaders (Fuchs et al., 2015; Pilkey et al., 2014). However, there are thunderstorms which exhibit a different, bottom-heavy, structure, where the lower positive layer is stronger than the upper positive layer (Bruning et al., 2014; Li et al., 2020; Marshall & Stolzenburg, 1998; Stolzenburg et al., 1998; Tesselndorf et al., 2007).

LOFAR, an array of radio antennas, is a software-based telescope used principally for astronomy research. Low-band antennas, grouped in stations in the Netherlands, operate in the 10–90 MHz frequency range and synchronize via atomic clocks with nanosecond stability. LOFAR is suitable for 3D localization of lightning sources with meters-scale accuracy (Scholten, Hare, Dwyer, Sterpka, et al., 2021) as well as for detecting cosmic-ray induced air showers (Buitink et al., 2014) since it is equipped with transient buffer boards that capture raw time traces.

Studying radio emissions of extensive air showers induced by cosmic rays provides an indirect method to determine the thundercloud electric fields. When an extensive shower passes through a thundercloud, its radio emission contains information about the cloud's electric field, enabling determination of both the field and thunderstorm charge distribution. This technique is applied at the LOFAR radio telescope, as detailed in Refs (Schellart et al., 2015; Trinh et al., 2020).

LOFAR is also capable of accurately imaging lightning discharges where lightning leaders measured at LOFAR show very different very high frequency (VHF) activity depending on their polarity. Propagating negative leaders can be most easily imaged due to strong VHF emission from their tips (Hare et al., 2020; Scholten, Hare, Dwyer, Liu, et al., 2021; Scholten et al., 2022). In contrast, positive leaders, though less VHF active at their tips, can be indirectly imaged through phenomena such as “needles” or “dart leaders” (Hare et al., 2019, 2021, 2023). From a LOFAR image, it is thus relatively easy to distinguish layers in the atmosphere where the discharge is dominated by negative or positive leaders which are clear signatures of positive and negative charge densities and follows previous work with LMA (Krehbiel et al., 1979; Pilkey et al., 2014).

One long-standing issue is that for thunderstorms imaged by LOFAR (called Dutch thunderstorms) using the lightning imaging technique, one consistently observes an upside-down structure compared to the large majority of thunderstorms measured in the world. LOFAR detects fewer cloud-to-ground lightning flashes compared to intra-cloud (IC) lightning. Furthermore, our lightning imaging data show that, in Dutch thunderstorms, the first leader seen after the initiation of a flash is generally directed downward from the negative charge layer, followed by a well-developed complex of negative leaders in the lower positive charge layer (Scholten, Hare, Dwyer, Sterpka, et al., 2021; Sterpka et al., 2021) while the usual structure seen around the world is one where at initiation the initial IC leader propagates upwards from the negative charge layer (Krehbiel et al., 1979; López et al., 2019; Marshall et al., 2005; Medina et al., 2021; Pu & Cummer, 2024; Williams, 1989; Zhang et al., 2023). Our present data suggest that this difference is due to a different charge buildup in thunderclouds. Contrary to the generally seen top-heavy structure, where the upper positive charge layer is stronger than the lower positive charge layer, it appears that Dutch thunderstorms show consistently a bottom-heavy structure where the lower layer contains more charge. This work aims to compare these results with the inferred thunderstorm charge structures derived from cosmic-ray measurements at LOFAR.

2. Charge Distribution Determination Using Extensive Air Showers

When a cosmic ray enters the upper layers of the atmosphere, it will collide with a particle in the atmosphere and generate many secondary particles. These particles form an extensive air shower. The number of particles in the air shower varies as a function of atmospheric depth. The depth where this number reaches a maximum is called X_{\max} . Most of the particles in the shower are electrons, positrons and photons. They move to the ground with a velocity near the speed of light. Due to the effect of the Lorentz force induced by the geomagnetic field, charged particles are deflected sideways from the shower direction. This forms a net transverse current pointing in the direction of the Lorentz force and this changing current emits radiation. This emission is linearly polarized along the direction of the current, the $\mathbf{v} \times \mathbf{B}$ direction where \mathbf{v} is the direction of the shower and \mathbf{B} that of the geomagnetic field (Scholten et al., 2018). In addition, electrons knocked out from the interaction between atmospheric and shower particles form an excess negative charge at the shower front. This also emits radio emission which is linearly polarized radially to the shower axis (Askaryan, 1962; de Vries et al., 2011). Under thunderstorm conditions, the electric field component perpendicular to the shower axis changes the current in both orientation

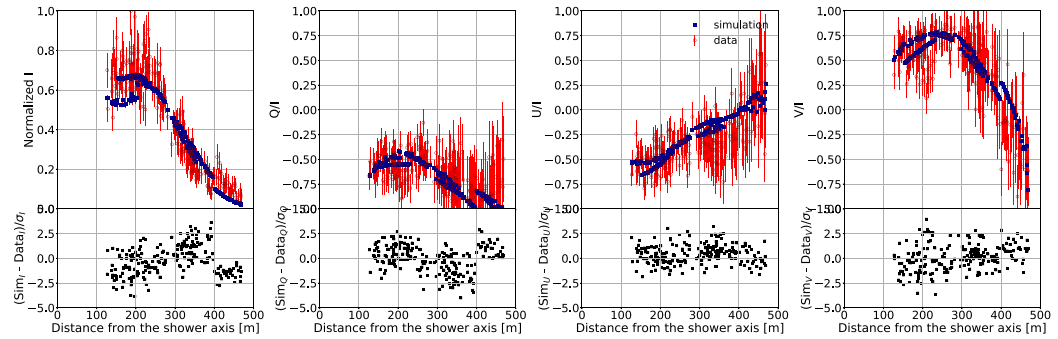


Figure 1. The normalized Stokes parameters (blue dots) calculated with CoREAS for the cosmic ray event are compared to LOFAR data (red circles). The bottom panel shows the difference between CoREAS and LOFAR data normalized by σ , the one standard deviation error.

and magnitude. Thus, the emission from the air shower is affected in both polarization and intensity (Trinh et al., 2016), reflecting the direction of the induced transverse current. As a result, the intensity and polarization footprints for the radio emission from an air shower measured under thunderstorm conditions, so-called thunderstorm events, are very different from the ones measured in fair-weather conditions, so-called fair-weather events (Schellart et al., 2015; Trinh et al., 2016). Therefore, one can determine the atmospheric electric fields in clouds based on the large effects on the footprints of the thunderstorm events.

Several thunderstorm events were recorded with LOFAR, a radio telescope with the core, so-called “Superterp” located near Exloo, in Drenthe in the Netherlands. In an offline analysis discussed in Schellart et al. (2013), the arrival direction and the energy of air showers are estimated. Additionally, the Stokes parameters, that carry the intensity and polarization information of the radio signal, are calculated for each antenna. Stokes I is the intensity of the radio emission. The linear polarization information is derived from Stokes Q and U . Stokes V is the intensity of the circularly polarized fraction of the radiation. In air showers measured under fair-weather conditions, radio signals are mainly polarized along the $\mathbf{v} \times \mathbf{B}$ direction which makes $Q/I \approx 1$ and $U/I \approx 1$. The amount of circular polarization seen in fair-weather events is also relatively small. In thunderstorm events, since the current changes between electric field layers, the Stokes parameters can have very different values, as can be seen in Figure 1, which clearly distinguishes it from a fair-weather shower.

In the period from June 2017 to April 2019, two thunderstorm cosmic-ray events were observed within 1 hr of LOFAR imaging a lightning flash. Here, we focus the event recorded on 21 September 2018 at 18:40:07 UTC.

To determine the electric fields, we solve the inverse problem based on chi-square fitting of the Stokes parameters. Using a steepest descent method, we optimize the parameters of the electric field structures by minimizing

$$\chi^2 = \sum_{\text{antenna}} \sum_{S=I}^{Q,U,V} \left(\frac{S_{k,C} - f S_{k,D}}{\sigma_k^2} \right)^2, \quad (1)$$

where $S_{k,C}$ are the Stokes parameters from calculations for antenna at position k and $S_{k,D}$ are the measured data from LOFAR. σ_k is the uncertainty and f is the normalization factor for the radio intensity. This procedure has been used in Trinh et al. (2020) where the radio footprint is fitted using a fast semi-analytic code, MGMR3D (Scholten et al., 2018). The fit parameters define the structure of the atmospheric electric fields. Since MGMR3D is based on certain approximations the extracted atmospheric electric field is used in a subsequent microscopic CoREAS (Huege et al., 2013) calculation. The comparison for the normalized Stokes parameters between CoREAS (Huege et al., 2013) and LOFAR data is shown in Figure 1. As can be seen, the features of the event are reconstructed rather well by the CoREAS simulation using the electric fields determined from MGMR3D (Scholten et al., 2018). The strength of the atmospheric electric fields, the heights where the fields change, the values of X_{max} and the values of χ^2 for this event are given in Table 1. The values for X_{max} differ for the CoREAS and the MGMR3D calculation. The reason for this is that for MGMR3D only the higher energy particles are important since they drive the radio emission while in CoREAS all particles are accounted for. To demonstrate that the fit shown in Figure 1 is the best one, we also perform simulations in which we varied the heights of the

Table 1
Nine Extracted Electric Field Parameters, X_{\max} and the Reconstructed Energy of the Event

h (km)	E (kV/m)	α (°)	E_z (kV/m)
6.6	50	62	−12
4.5	91	67	53
3.6	98	123	18
MGMR3D		CoREAS	
X_{\max} (g/cm ²)	643	759	
Energy (GeV)	3.17×10^7	2.12×10^8	
χ^2	1.0	1.3	

layers by 0.5 km and the strengths of the electric fields by 30% of the initial values. All these fits, which can be found in Supporting Information S1, have larger values of χ^2 than the one of the fit shown in Figure 1.

As can be seen from Figure 1, the values of the Stokes parameters for this thunderstorm event are significantly different from those of fair-weather events. The heights h and angles α relative to the $\mathbf{v} \times \mathbf{B}$ direction of the electric fields can be inferred from the Stokes parameters. At distances between 400 and 500 m from the shower axis, the radio emission mainly originates from high altitudes. In this region, the polarization ratio is characterized by $Q/I \approx -1$ and $U/I \approx 0$. This implies that the polarization direction, and therefore the induced transverse current at these altitudes, is perpendicular to that observed in fair weather showers, indicating $\alpha \approx 90^\circ$ or $\alpha \approx 210^\circ$. However, as shown in Table 1, α is determined to be 62° . This discrepancy is due to the fact that the direction of the transverse current is

influenced by the net force, the combination of the Lorentz force and the electric force. In the distance range from 250 to 300 m from the core, the direction changes, indicative of a layer boundary at an altitude of about 4.5 km. At any distance the spread in linear as well as circular, V/I , polarization is relatively small, as compared to fair weather events, indicating that the electric fields are rather strong and thus suppressing the influence of charge-excess radiation. The large values for V/I at distances from 150 till 350 m indicate that there are about equal contributions to the signal from different emission heights and orientations.

The cosmic-ray measurements are sensitive only to the components orthogonal to the shower axis, given in the column E in Table 1. The electric field component aligned with the shower axis, E_v , affects the production of electrons or positrons based on its polarity. However, because the particles generated by E_v have relatively low energies, they fall significantly behind the shower front (Trinh et al., 2016). This results in the radio emissions from these particles contributing coherently only at lower frequencies, under 10 MHz, which are lower than the range from 30 to 80 MHz that the LOFAR can detect (Trinh et al., 2016). Therefore, LOFAR does not have sensitivity to E_v and we assume that $E_v = 0$. Since generally the charge layers in clouds are horizontal (Rust et al., 2005) (from images of lightning discharges, such as presented later in this work, it can be seen that angles up to 10° are not uncommon) we want to infer the vertical component of the electric field, E_z pointing vertically up, given in the column E_z in Table 1.

From the vertical electric field component E_z , we can determine the charge distribution of the thundercloud where the event passed through. The charge density of the cloud $\rho_{i,i+1}$ between the electric field layer i and layer $i + 1$ is derived from

$$E_{z,i} - E_{z,i+1} = \frac{\rho_{i,i+1}}{\epsilon_0}, \quad (2)$$

where $E_{z,i}$ for different layers is shown in Table 1 and $\epsilon_0 = 8.85 \times 10^{-12} \text{ Fm}^{-1}$. For simplicity we assume that the field above the top layer vanishes. The heights indicated by the present analysis can be considered as the average heights of the charge layers. There are positive charged layers at 6.6 and 3.6 km and a negative one at 4.5 km, as shown in Figure 2. The magnitudes of the surface charge density in the top and the bottom layer are $1.06 \times 10^{-7} \text{ C/m}^2$ and $3.10 \times 10^{-7} \text{ C/m}^2$, respectively. That of the middle charge layer is $-5.75 \times 10^{-7} \text{ C/m}^2$. These magnitudes are comparable to the results derived from balloon soundings of electric fields in small New Mexican mountain thunderstorms shown in Marshall and Stolzenburg (1998). Previous lightning-imaging work by our group had already suggested a bottom-heavy charge structure, with the lower positive being stronger than the upper positive (Scholten, Hare, Dwyer, Sterpka, et al., 2021; Sterpka et al., 2021), which is confirmed by this work. This is different from the majority of thunderstorms seen around the world. We hypothesize that this is due to the northern latitudes and the sea climate in the Netherlands. The troposphere usually lies at about 10 km altitude, which, combined with the sea climate, makes that most Dutch thunderstorms are much less severe. The much weaker updrafts could be the cause of less efficient charging of the top layer and thus be the reason for the bottom-heavy charge distributions. It is tempting to sum the three charge densities to arrive at some kind of average charge density of the storm. However, cosmic ray air showers are very thin relative to the size of the

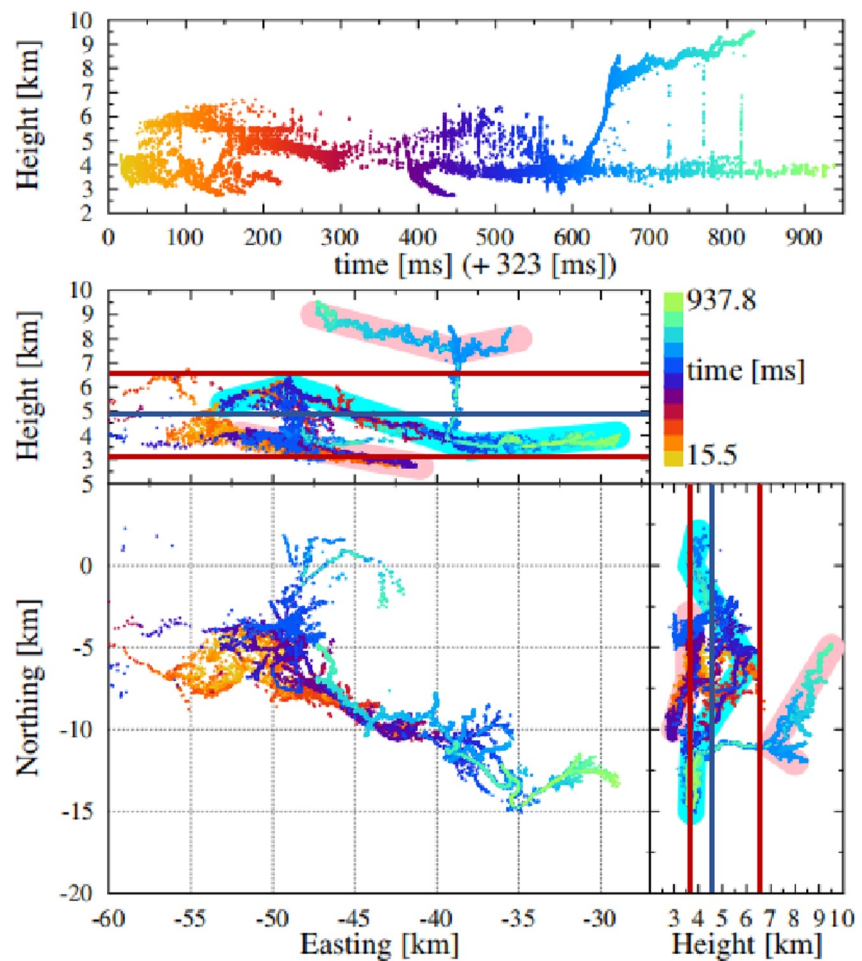


Figure 2. Image of the lightning flash. The Northing and Easting coordinates are given with respect to the LOFAR-core. Schematically the positive (negative) charge layers are indicated in pink (blue). The heights of the positive (negative) charge layers determined by the air-shower event are indicated by the red (blue) lines.

storm. Thus our results effectively measure the electric fields along a thin line through the storm. Therefore, complicated storm dynamics, such as wind-shear, can easily cause the charge density measured at a point (like ours) to be different from the average charge density of the storm.

3. Charge Distribution Determination Using Lightning Imaging

Around the time of the cosmic-ray event there were also LOFAR recordings for the purpose of imaging lightning discharges. The images show positive and negative leaders (among other aspects of the discharge) that proceed through negative and positive charge layers. On the LOFAR images they can be distinguished by the fact that negative leaders show many imaged sources at their propagating fronts while the active fronts of positive leaders are not visible on LOFAR images (Scholten et al., 2023), instead the needle activity is seen along the leaders (Hare et al., 2018). These needles are very intermittent and are less dense in their imaged sources than negative leaders.

About an hour after the cosmic-ray event occurred (at 19:42:59 UTC) a lightning discharge was recorded with LOFAR shown in Figure 2. As can be seen from the image of the flash, in particular from the panel showing height versus Easting (although some aspects need a more detailed zoom-in to distinguish), there is a complex of negative leaders schematically indicated in pink showing that there is a slanted layer of positive charge at the lowest altitudes. At somewhat higher altitudes there is a layer of negative charge indicated in blue that is evidenced by a complex of positive leaders. At much higher altitudes a complex of high altitude negative leaders

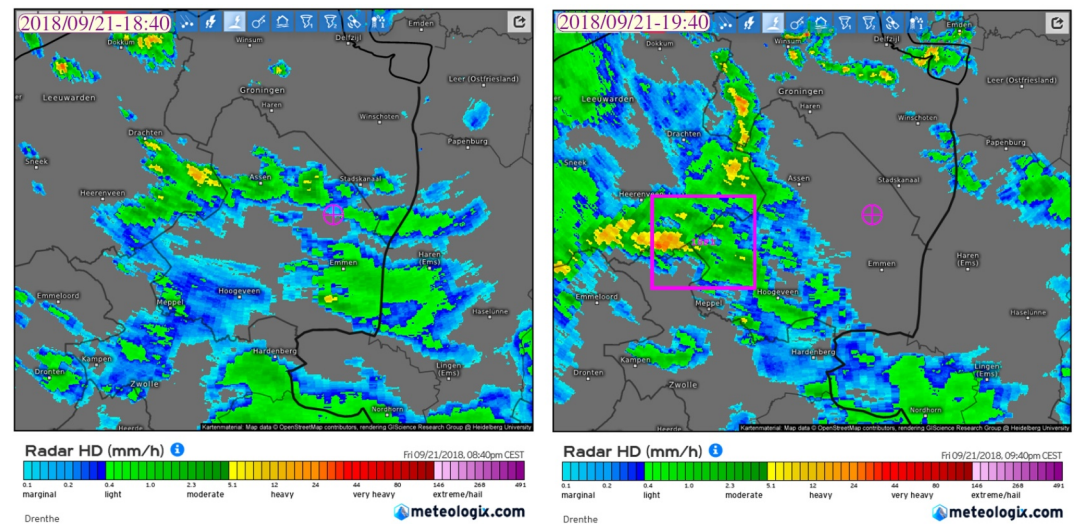


Figure 3. Rainfall (meteologix.com, 2023) over the LOFAR area left at 21 September 2018 at 18:40 UTC, the time of the cosmic-ray detection, right at 19:40, the same day, 3 min before the lightning flash given in Figure 2 was recorded. The core of LOFAR is indicated by the magenta \oplus and the magenta square on the right denotes the size of the ground-projection pane in Figure 2.

(HANL's) (Scholten, Hare, Dwyer, Liu, et al., 2021) is seen indicating another slightly slanted positive charge layer (pink). These HANL's are fed by a few dart leaders that are initiated from the positive leader at 4 km altitude, confirming the opposite charges of these layers. The density of negative leaders in the lower layer is larger than in upper layer which can be seen as evidence that the lower positive charge layer is stronger than the upper one. An interesting aside is that from the ground projection shown in Figure 2 it is seen that all leaders stretching south-east from the lightning initiation site lie almost straight above each other, spread over altitudes ranging from 3 till 9 km. The charge layers may thus have the structure of bands with a length that is 10 times larger than the width.

Figure 3 gives the cloud cover over the LOFAR area close to the times when the cosmic-ray event and the lightning flash were recorded. In relating the charge distribution one should realize that the clouds move eastward at close to 100 km/hr. This can be seen best by displaying the frames at intermediate times from the ones shown in Figure 3, showing that the most intense rainfall at the time of the cosmic-ray recording (the larger yellow-orange structure on the left) moved to the large green cloud at the right corner of the right pane in Figure 3. According to SEVIRI satellite data (Meirink et al., 2022), at the time of the cosmic ray measurement the cloud top height over the LOFAR core were at a moderate height of about 7 km.

It is tempting to compare quantitatively the charge structures determined from the cosmic-ray observation and from the imaged flash even though the lightning discharge as recorded by LOFAR (at 19:42:59 UTC) occurred an hour later than the cosmic-ray event and at a different location. Since the countryside is flat and storms propagate over hundreds of kilometers one would expect the same general structure for flashes in the same storm, as is supported by comparing images of different flashes in the same storm. The observed charge structures from cosmic-ray measurement and from lightning imaging exhibit similarities. Both measurements suggest a triple charge layer, with a main negative layer between the upper positive and lower positive layers, with a negative charge layer at a moderately high altitude, at 4.5 km, with positive charge layers above and below. This might suggest that the subsequent convective cells, the first struck by the cosmic-ray, and the second struck by a lightning discharge, are the result of similar storm dynamics, resulting in a similar charge distribution. It should be noted that the altitudes of the charge layers determined by the lightning flash are location dependent, whereas those derived from the cosmic-ray event are determined at a single location, the LOFAR core. The similar features observed using both methods, imply that the charge density, which cannot be obtained from lightning imaging but can be inferred from cosmic-ray events, might be reliable.

4. Conclusion

In this work, we show the unique capabilities of LOFAR to perform two distinct types of observations, testing their consistency. The thunderstorm charge layer structure as inferred from lightning imaging with that as determined from a cosmic-ray measurement both show triple charge layer, with a main negative layer between two positive layers where the lower positive layer has a larger charge than the upper one. Our results even show a general agreement between the heights of the charge structure determined by the two methods. Consequently, the charge density insights gained from cosmic-ray observations could potentially be useful in enhancing our understanding of lightning, though further studies are needed to confirm this. From Figure 2 we observe that the layer with more charge supports a larger density of negative leaders and thus show more VHF activity. This leads to the postulate that number of VHF pulses is a proxy for the amount of cloud charge, which should be investigated in future work.

Data Availability Statement

- Data:
 - Data set Data-275251207.dat from ref. (Trinh, 2024) contains the information about the cosmic ray event, including the event number, azimuth and zenith angles, antenna positions, Stokes parameters, and their uncertainties. Stokes parameters as is used in Figure 1.
 - Data set 18F1o18SW-all.dat from ref. (Trinh, 2024) lists the data on the lightning flash given in Figure 2, with columns for a unique source label, time, and source position.
 - The data on rain-clouds, Figure 3, were obtained from using (meteologix.com, 2023).
- Software:
 - To determine the atmospheric electric fields from the radio emission from a cosmic-ray air shower the code MGMR3D was used (Scholten, 2023)
 - The plotting package GLE (Pugmire et al., 2015) was used for making Figure 2.

Acknowledgments

BMH and PT are supported ERC Grant Agreement No. 101041097. SBo, AN, and KT acknowledge the Verbundforschung of the German Ministry for Education and Research (LOFAR-ERIC, ErUM-IFT). PL is supported by the German Research Foundation (DFG)—Project 531213488.

References

- Askaryan, G. (1962). Excess negative charge of the electron-photon shower and coherent radiation originating from it. Radio recording of showers under the ground and on the Moon. *Journal of the Physical Society of Japan*, 17(Suppl), 257.
- Bruning, E. C., Weiss, S. A., & Calhoun, K. M. (2014). Continuous variability in thunderstorm primary electrification and an evaluation of inverted-polarity terminology. *Atmospheric Research*, 135–136, 274–284. <https://doi.org/10.1016/j.atmosres.2012.10.009>
- Buitink, S., Corstanje, A., Enriquez, J., Falcke, H., Hörandel, J., Huege, T., et al. (2014). Method for high precision reconstruction of air shower X_{\max} using two-dimensional radio intensity profiles. *Physical Review D*, 90(8), 082003. <https://doi.org/10.1103/PhysRevD.90.082003>
- de Vries, K. D., van den Berg, A. M., Scholten, O., & Werner, K. (2011). Coherent Cherenkov radiation from cosmic-ray-induced air showers. *Physical Review Letters*, 107(6), 061101. <https://doi.org/10.1103/PhysRevLett.107.061101>
- Dwyer, J. R., & Uman, M. A. (2014). The physics of lightning. *Physics Reports*, 534(4), 147–241. <https://doi.org/10.1016/j.physrep.2013.09.004>
- Fuchs, B. R., Rutledge, S. A., Bruning, E. C., Pierce, J. R., Kodros, J. K., Lang, T. J., et al. (2015). Environmental controls on storm intensity and charge structure in multiple regions of the continental United States. *Journal of Geophysical Research: Atmospheres*, 120(13), 6575–6596. <https://doi.org/10.1002/2015JD023271>
- Hare, B. M., Scholten, O., Bonardi, A., Buitink, S., Corstanje, A., Ebert, U., et al. (2018). LOFAR lightning imaging: Mapping lightning with nanosecond precision. *Journal of Geophysical Research: Atmospheres*, 123(5), 2861–2876. <https://doi.org/10.1002/2017JD028132>
- Hare, B. M., Scholten, O., Buitink, S., Dwyer, J. R., Liu, N., Sterpka, C., & ter Veen, S. (2023). Characteristics of recoil leaders as observed by LOFAR. *Physical Review D*, 107(2), 023025. <https://doi.org/10.1103/PhysRevD.107.023025>
- Hare, B. M., Scholten, O., Dwyer, J., Ebert, U., Nijdam, S., Bonardi, A., et al. (2020). Radio emission reveals inner meter-scale structure of negative lightning leader steps. *Physical Review Letters*, 124(10), 105101. <https://doi.org/10.1103/PhysRevLett.124.105101>
- Hare, B. M., Scholten, O., Dwyer, J., Sterpka, C., Buitink, S., Corstanje, A., et al. (2021). Needle propagation and twinkling characteristics. *Journal of Geophysical Research: Atmospheres*, 126(6), e2020JD034252. <https://doi.org/10.1029/2020JD034252>
- Hare, B. M., Scholten, O., Dwyer, J., Trinh, T. N. G., Buitink, S., ter Veen, S., et al. (2019). Needle-like structures discovered on positively charged lightning branches. *Nature*, 568(7752), 360–363. <https://doi.org/10.1038/s41586-019-1086-6>
- Huege, T., Ludwig, M., & James, C. W. (2013). Simulating radio emission from air showers with CoREAS. *AIP Conference Proceedings*, 1535(1), 128–132. <https://doi.org/10.1063/1.4807534>
- Krehbiel, P. R., Brook, M., & McCrory, R. A. (1979). An analysis of the charge structure of lightning discharges to ground. *Journal of Geophysical Research*, 84(C5), 2432–2456. <https://doi.org/10.1029/JC084iC05p02432>
- Li, Y., Zhang, G., & Zhang, Y. (2020). Evolution of the charge structure and lightning discharge characteristics of a Qinghai-Tibet Plateau thunderstorm dominated by negative cloud-to-ground flashes. *Journal of Geophysical Research: Atmospheres*, 125(5), e2019JD031129. <https://doi.org/10.1029/2019JD031129>
- López, J. A., Montanyà, J., van der Velde, O. A., Pineda, N., Salvador, A., Romero, D., et al. (2019). Charge structure of two tropical thunderstorms in Colombia. *Journal of Geophysical Research: Atmospheres*, 124(10), 5503–5515. <https://doi.org/10.1029/2018JD029188>
- Marshall, T. C., & Stolzenburg, M. (1998). Estimates of cloud charge densities in thunderstorms. *Journal of Geophysical Research*, 103(D16), 19769–19775. <https://doi.org/10.1029/98JD01674>
- Marshall, T. C., Stolzenburg, M., Maggio, C. R., Coleman, L. M., Krehbiel, P. R., Hamlin, T., et al. (2005). Observed electric fields associated with lightning initiation. *Geophysical Research Letters*, 32(3), L03813. <https://doi.org/10.1029/2004GL021802>

- Medina, B. L., Carey, L. D., Lang, T. J., Bitzer, P. M., Deierling, W., & Zhu, Y. (2021). Characterizing charge structure in central Argentina thunderstorms during relampago utilizing a new charge layer polarity identification method. *Earth and Space Science*, 8(8), e2021EA001803. <https://doi.org/10.1029/2021EA001803>
- Meirink, J. F., Karlsson, K.-G., Solodovnik, I., Hüser, I., Benas, N., Johansson, E., et al. (2022). CLAAS-3: CM SAF CLoud property dAtAset using SEVIRI - Edition 3. In *Satellite Application Facility on Climate Monitoring (CM SAF)*. https://doi.org/10.5676/EUM_SAF_CM/CLAAS/V003
- meteologix.com. (2023). meteologix. Retrieved from <https://meteologix.com/>
- Pilkey, J. T., Uman, M. A., Hill, J. D., Ng, T., Gamarota, W. R., Jordan, D. M., et al. (2014). Rocket-triggered lightning propagation paths relative to preceding natural lightning activity and inferred cloud charge. *Journal of Geophysical Research: Atmospheres*, 119(23), 13427–13456. <https://doi.org/10.1002/2014JD022139>
- Pu, Y., & Cummer, S. A. (2024). Continuous initial breakdown development of in-cloud lightning flashes. *Journal of Geophysical Research: Atmospheres*, 129(20), e2024JD041302. <https://doi.org/10.1029/2024JD041302>
- Pugmire, C., Mundt, S. M., LaBella, V. P., & Struyf, J. (2015). Graphics layout engine GLE 4.2.5 user manual [Software]. *GLE*. Retrieved from <https://glx.sourceforge.io/index.html>
- Rakov, V. A., & Uman, M. A. (2007). *Lightning: Physics and effects*. Cambridge University Press.
- Rust, W. D., MacGorman, D. R., Bruning, E. C., Weiss, S. A., Krehbiel, P. R., Thomas, R. J., et al. (2005). Inverted-polarity electrical structures in thunderstorms in the Severe Thunderstorm Electrification and Precipitation Study (STEPS). *Atmospheric Research*, 76(1), 247–271. <https://doi.org/10.1016/j.atmosres.2004.11.029>
- Rutledge, S. A., Williams, E. R., & Petersen, W. A. (1993). Lightning and electrical structure of mesoscale convective systems. *Atmospheric Research*, 29(1), 27–53. [https://doi.org/10.1016/0169-8095\(93\)90036-N](https://doi.org/10.1016/0169-8095(93)90036-N)
- Schellart, P., Nelles, A., Buitink, S., Corstanje, A., Enriquez, J. E., Falcke, H., et al. (2013). Detecting cosmic rays with the LOFAR radio telescope. *Astronomy & Astrophysics*, 560, A98. <https://doi.org/10.1051/0004-6361/201322683>
- Schellart, P., Trinh, T., Buitink, S., Corstanje, A., Enriquez, J., Falcke, H., et al. (2015). Probing atmospheric electric fields in thunderstorms through radio emission from cosmic-ray-induced air showers. *Physical Review Letters*, 114(16), 165001. <https://doi.org/10.1103/PhysRevLett.114.165001>
- Scholten, O. (2023). MGMR3D [Software]. *Zenodo*. <https://doi.org/10.5281/zenodo.7698097>
- Scholten, O., Hare, B., Dwyer, J., Liu, N., Sterpka, C., Buitink, S., et al. (2021a). Distinguishing features of high altitude negative leaders as observed with LOFAR. *Atmospheric Research*, 260, 105688. <https://doi.org/10.1016/j.atmosres.2021.105688>
- Scholten, O., Hare, B. M., Dwyer, J., Liu, N., Sterpka, C., Kolmasová, I., et al. (2022). Interferometric imaging of intensely radiating negative leaders. *Physical Review D*, 105(6), 062007. <https://doi.org/10.1103/PhysRevD.105.062007>
- Scholten, O., Hare, B. M., Dwyer, J., Liu, N., Sterpka, C., Mulrey, K., & Veen, S. T. (2023). Searching for intra-cloud positive leaders in VHF. *Scientific Reports*, 13(1), 14485. <https://doi.org/10.1038/s41598-023-41218-x>
- Scholten, O., Hare, B. M., Dwyer, J., Sterpka, C., Kolmasova, I., Santolik, O., et al. (2021b). The initial stage of cloud lightning imaged in high-resolution. *Journal of Geophysical Research: Atmospheres*, 126(4), e2020JD033126. <https://doi.org/10.1029/2020JD033126>
- Scholten, O., Trinh, T. N. G., de Vries, K. D., & Hare, B. M. (2018). Analytic calculation of radio emission from parametrized extensive air showers: A tool to extract shower parameters. *Physical Review D*, 97(2), 023005. <https://doi.org/10.1103/PhysRevD.97.023005>
- Sterpka, C., Dwyer, J., Liu, N., Hare, B. M., Scholten, O., Buitink, S., et al. (2021). The spontaneous nature of lightning initiation revealed. *Geophysical Research Letters*, 48(23), e2021GL095511. <https://doi.org/10.1029/2021GL095511>
- Stolzenburg, M., Rust, W. D., & Marshall, T. C. (1998). Electrical structure in thunderstorm convective regions: 2. Isolated storms. *Journal of Geophysical Research*, 103(D12), 14079–14096. <https://doi.org/10.1029/97JD03547>
- Tessendorf, S. A., Wiens, K. C., & Rutledge, S. A. (2007). Radar and lightning observations of the 3 June 2000 electrically inverted storm from steps. *Monthly Weather Review*, 135(11), 3665–3681. <https://doi.org/10.1175/2006MWR1953.1>
- Trinh, T. N. G. (2024). Thunderstorm charge distribution determination using cosmic rays induced air showers and lightning imaging at LOFAR [Dataset]. *Zenodo*. <https://doi.org/10.5281/zenodo.13892214>
- Trinh, T. N. G., Scholten, O., Buitink, S., Ebert, U., Hare, B. M., Krehbiel, P. R., et al. (2020). Determining electric fields in thunderclouds with the radiotelescope LOFAR. *Journal of Geophysical Research: Atmospheres*, 125(8), e2019JD031433. <https://doi.org/10.1029/2019JD031433>
- Trinh, T. N. G., Scholten, O., Buitink, S., van den Berg, A., Corstanje, A., Ebert, U., et al. (2016). Influence of atmospheric electric fields on the radio emission from extensive air showers. *Physical Review D*, 93(2), 023003. <https://doi.org/10.1103/PhysRevD.93.023003>
- Williams, E. R. (1989). The tripole structure of thunderstorms. *Journal of Geophysical Research*, 94(D11), 13151–13167. <https://doi.org/10.1029/JD094iD11p13151>
- Zhang, H., Zhang, Y., Fan, Y., Zhang, Y., Krehbiel, P. R., & Lyu, W. (2023). Guangdong lightning mapping array: Errors evaluation and preliminary results. *Earth and Space Science*, 10(11), e2023EA003143. <https://doi.org/10.1029/2023EA003143>